Comparison of the properties of laser-driven x-ray sources to existing compact x-ray sources

Contact: dan.symes@stfc.ac.uk

D. R. Symes
Central Laser Facility,
STFC Rutherford Appleton Laboratory,
Chilton, Didcot, OX11 0QX

J. M. Cole, J. C. Wood, S. P. D. Mangles, & Z. Najmudin
The John Adams Institute for Accelerator Science,
Blackett Laboratory, Imperial College London,
London SW7 2AZ

N. C. Lopes
The John Adams Institute for Accelerator Science,
Blackett Laboratory, Imperial College London,
London SW7 2AZ
& GoLP/Instituto de Plasmas e Fusão Nuclear,
Instituto Superior Técnico,
U.L., Lisboa 1049-001, Portugal

Abstract

Compact x-ray sources with much higher brightness than conventional electron-impact x-ray tubes are being developed to translate the advanced techniques achievable at synchrotron beamlines to laboratory settings. The benefits for biological research will be faster scanning at very high resolution for rapid μCT and in vivo studies. X-ray sources based on relativistic electron beams produced in miniature plasma accelerators driven by high power lasers have ideal properties for these applications of micron-scale source size, extreme brightness and ultrashort image exposure time. The lateral coherence of the beam enables phase contrast imaging, providing superior contrast between soft tissues compared to traditional absorption-based radiography. The purpose of this report is to compare the performance of plasma accelerator based x-ray technology to other options available to researchers and discuss future capabilities.

1 Introduction

X-ray micro-computed tomography (μCT) [1] is useful for non-invasive biological imaging because it has high spatial resolution and greater depth penetration than optical techniques. Critical factors for x-ray imaging are image contrast, spatial resolution, total acquisition time and dose. The choice of x-ray equipment depends on the source parameters that are most important for the particular application, and is also determined by the budget of the research activity. While the majority of x-ray imaging relies on absorption, superior distinction between soft tissues can be attained by employing x-ray phase contrast imaging [2, 3, 4, 5] that detects the slight deflections of x-rays caused by density gradients at the material boundaries.

Conventional x-ray sources operate by irradiating an anode material with an electron beam generating K_α line emission and broad bandwidth bremsstrahlung radiation. Being a mature technology, x-ray tube devices are widely used and cover a range of imaging parameters. Commercial μCT machines can deliver full body small animal scanning in less than one minute [6], phase contrast capability [7, 8, 9, 10, 11] and sub-μm resolution [12, 13], but not all from a single machine. Their brightness is limited by the heat load on the anode leading to a trade-off between x-ray source size and acquisition speed. At extremely high resolution, long exposure times are required, making live animal imaging difficult. At the other end of the scale, researchers can use synchrotron light sources [lightsources.org] that are many orders of magnitude brighter than x-ray tubes. Using dedicated beamlines with high frame rate detectors (up to 1000s of frames per second) x-ray μCT can be carried out in a few seconds. This much shorter acquisition time allows imaging of fast biological processes with μm-level spatial resolution [14, 15, 16, 17]. Because their infrastructure is on the scale of a national facility, access to synchrotrons is limited, leading to a strong motivation to develop innovative technologies to fill this gap and provide advanced imaging capabilities with compact devices [18]. In this report, we compare the source properties of some commercial systems to the capabilities of laser-driven sources.

2 X-ray sources based on laser-plasma accelerators

Laser-driven light-sources offer a high brightness solution with a size and cost compatible with future deployment in standard laboratory or clinical environments. These sources are based on a miniature laser plasma accelerator (LPA) [19, 20, 21, 22] created by focussing a high power (> 100 TW), ultrashort (~ 40 fs) laser pulse through a gas target. As the intense pulse propagates it ionises the gas and creates an extremely strong accelerating field in which trapped electrons can reach high energies (> 1 GeV) within a short distance (~ 10mm) [23, 24, 25]. The electrons undergo oscillations in the plasma, termed betatron oscillations, emitting an extremely bright pulse of x-ray radiation in the forward direction with a μm-scale

x-ray source size [26, 27, 28, 29]. Because the accelerating gradients of 100 GV m^{-1} are so much higher than the 100 MV m^{-1} limit of conventional technology the accelerator is correspondingly smaller. In addition, the small source size means that in distances of order 1 m they achieve the same degree of lateral coherence as synchrotron beamlines 100 times longer. The laser-betatron photon flux can be $> 10^{10}$ photons per pulse in a broad synchrotron-like energy spectrum with a critical energy in the range 5 - 450 keV depending on laser parameters [30, 31, 32, 33, 34]. X-rays can also be generated by colliding a second laser pulse with the relativistic electron bunch [35]. The laser photons backscatter (termed Inverse Compton Scattering (ICS)) in the direction of the electron beam and gain a factor of $4\gamma^2$ in energy, where γ is the relativistic factor of the electrons. This all-optical ICS source can generate $> 10^7$ photons per pulse [36]. X-ray beams in the tens of keV region suitable for biological imaging have been produced from tens of MeV electron beams accessible with modest laser energies ($\sim$1 J) [36, 37]. The properties of these LPA sources of short pulse duration (< 100 fs), small source size ($\sim 1\mu$m), extreme brightness ($10^7 - 10^{10}$ x-ray photons per laser pulse) and a high degree of spatial coherence are ideal for the application of high resolution phase enhanced x-ray μCT [31, 32, 33, 38, 39].

3 Other compact x-ray source technologies

3.1 K_α and bremsstrahlung sources

The highest power benchtop electron-impact x-ray sources are based on liquid metal anodes [40], such as the *MetalJet*, manufactured by Excillum AB [excillum.com]. These sources operate with gallium alloys with a low melting point, with an x-ray spectrum dominated by the Ga K_α line at 9 keV. Increasing the indium content raises the photon energy to 24 keV [41] at the expense of a more complicated design due to the higher melting point of the alloy. The limiting factor on brightness is evaporation of the metal anode by the electron beam [42]. Higher power loading can be applied if the speed of the jet is increased and the x-ray yield has been shown on a prototype machine to be linear with electron power up to $\sim$ 200 W ($\sim$ 10 MW mm^{-2}) [43]. Direct laser irradiation of a solid [44, 45] or liquid [46, 47] target can also be used to generate K_α radiation for imaging. A 100 Hz laser-driven K_α Mo source was recently developed at the LP3 laser facility [lp3.univ-mrs.fr/] [48]. This has very high flux, but because of rapid heat transport in the plasma the x-ray emission region is larger ($\sim$10 μm) than the laser focal spot size which will limit image resolution.

Commercial liquid anode μCT machines are capable of phase contrast imaging [49, 50, 51, 52] and tomography with resolution in the few-10 μm range within 30 seconds [53]. Higher resolution imaging ($< 5\mu$m) has shown sub-cellular features in muscle structure [54] and neuronal tissue [55] but with longer single-image exposures of $\sim$100 seconds. The clear advantage of the *MetalJet* is its low cost, small size and relative simplicity, meaning it can easily be adopted by laboratories already familiar with conventional μCT machines. However, it is not easily tunable because the x-ray emission is dependent on the anode material and for live imaging at the highest resolutions, the x-ray flux needs to increase by at least a factor of 10.

3.2 Table-top synchrotrons

Compact devices can be built by incorporating conventional (radio frequency, RF) electron accelerator technology but ensuring a small footprint. The Paul Scherrer Institute have designed 10m x 5m synchrotrons operating up to 20 keV with a view to commercialisation [aa-t.ch/]. By including a metal target in a tabletop synchrotron, the Photon Production Laboratory [photon-production.co.jp] produce high brightness bremsstrahlung radiation over a large range of energies [56, 57]. In this scheme, marketed as the *Mirrorcle*, a small x-ray source size is achieved by limiting the size of the convertor, although this leads to a trade off between source size and flux. The capabilities of the machine for biological and clinical imaging have been reported [58].

3.3 RF accelerator Inverse Compton sources

ICS can be used to produce x-ray sources based on RF accelerators with relatively modest electron energies of tens of MeV [59, 60, 61]. This is achievable in a footprint of several metres with a modern accelerator. A counter-propagating laser is precisely synchronised to the electron beam and both beams are tightly focussed at the collision point. X-rays are emitted in a beam with about 10^{10} photons per second in a narrow bandwidth (few %) which is tuneable by changing the electron energy. Compact storage ring accelerators can achieve very high repetition rates (MHz) but compared to a linear accelerator have a longer electron bunch length. This can improve the stability of the machine but also leads to a larger x-ray source size because the laser depth of focus must be comparable to the bunch length to maximise the colliding efficiency. Therefore ring-based designs have an x-ray source size of $\sim$ 30 μm [60] whereas linac-based designs have $\sim$ 2 μm [61].

This technology has been developed as a commercial system – the *Compact Light Source* (CLS) – by Lyncean Technologies Inc. [lynceantech.com]. The first *CLS* was installed at the Technical University of Munich in 2015 [62, 63] and delivers $\sim 10^{10}$ photons s^{-1} in a beam with 4 mrad divergence. The detector is placed 16 m from the source providing a 6 cm field of view. The single image acquisition time is typically of order 1 second [64] but adequate SNR can be achieved with exposures as

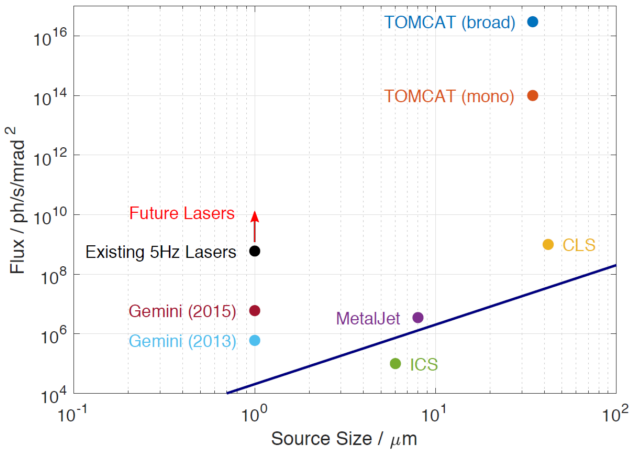

Figure 1: Flux of compact x-ray sources plotted against the x-ray source size. Values for the *MetalJet* (purple circle) and the *Compact Light Source* (yellow circle) are shown as listed in table 1. Parameters of the TOMCAT beamline (broad bandwidth: blue circle; 2% bandwidth: brown circle) and a simulated limit to solid anode tungsten sources (blue line) are included for comparison. Laser-based ICS sources (green circle) with 10^7 ph s^{-1} have been demonstrated corresponding to 10^5 ph s^{-1} mrad^{-2} at 10 Hz. The laser-betatron source size is of order 1 μm and in this work we achieved a flux 6×10^6 ph s^{-1} mrad^{-2} at low repetition rate. Existing lasers operating at 5 Hz could increase this flux to 6×10^8 ph s^{-1} mrad^{-2} and developments in the near future could reach $> 10^{10}$ ph s^{-1} mrad^{-2}.

short as 50 ms [65], needed for in vivo imaging [66]. The key benefit of the *CLS* is its intrinsic monochromaticity [67, 68] which can lower dose and is preferred for grating based phase contrast imaging. The x-ray photon energy is easily tuneable and in the current machine reaches a maximum of 35 keV [62]. A drawback is that the x-ray source size of 42 μm is large compared to other microfocus sources and this cannot be made much smaller in a ring-based design.

4 Comparison of bright compact x-ray sources

The parameters of LPA x-ray sources are shown in table 1 and figure 1 alongside those of other bright compact x-ray sources currently available. This allows a comparison in terms of photon brightness, image acquisition time and x-ray source size. For context we have included the parameters of the PSI TOMCAT synchrotron beamline [psi.ch/sls/tomcat/] that is dedicated to tomographic imaging [15, 69], and a plot of the calculated limit for solid tungsten anode x-ray emission [32].

The major advantage of LPA sources is that the x-ray source size is inherently small and *remains microscopic* when the drive laser power increases. For betatron radiation, the source size is set by the dimensions of the plasma wakefield structure and for laser-ICS it is determined by the μm-scale focus of the intense colliding laser. Inferred betatron source sizes of order 1 - 2 μm [31, 33] are significantly lower than the other sources and provide good spatial coherence in a short distance. In common with the *CLS* the x-ray beam has low divergence, allowing imaging at a distance and straightforward implementation of propagation-based phase contrast imaging [65] without a high loss in x-ray flux. Both LPA source schemes are capable of reaching higher photon energies than is currently available with the *Metaljet* or the *CLS*. Tuning to a higher photon energy range ($>$ 50 keV) is necessary for denser objects such as bone [32] and could reduce dose in clinical phase contrast imaging [2]. A unique feature of high-power laser-driven sources is their ultrashort duration (sub-ps). Although the other sources have high *average* flux, they have lower *peak* flux meaning that the image signal-to-noise ratio worsens as the detector exposure time is reduced [65]. In contrast, the laser-driven x-ray duration is always much shorter than the exposure time, so this can be minimised with no detrimental effect on the image quality. This also means that the acquisition rate is not source limited, but rather is determined by the repetition rate of the laser and the frame rate of the camera.

In our current work, the low repetition rate of the Gemini laser (0.05 Hz) was a drawback, lowering the average photon flux to $\sim 6 \times 10^6$ ph s^{-1} mrad^{-2}. To record 360 projections for tomographic scanning required 2 hours of beam time. Growth in this research area has led to commercialisation and a proliferation of compact high power laser systems with a size and cost ($\sim$ 2M Euro) manageable by research groups [72]. A consequence of an industrial approach to the production of these laser systems is an improvement in their robustness and consistency making them suitable for deployment as dedicated x-ray imaging machines. Laser-betatron and laser-ICS x-ray beams can be generated with laser pulse energies $<$ 10 J and such systems are already operational with repetition rates at 5 - 10 Hz (for more information see the interactive world map of laser capabilities maintained by the International Committee on Ultra-High Intensity Lasers: lasers.llnl.gov/map/index.htm). Tomographic scanning within a few minutes (images acquired at 1 f.p.s.) has recently been demonstrated [38] and we do not envisage any technical barriers to increasing the x-ray output to $\sim 10^{11}$ photons s^{-1} with existing laser systems. Furthermore, a shift to diode-pumped solid state technology [73, 74] offers scalability in power and repetition rate beyond current capabilities. Alternative approaches to laser wakefield acceleration [75, 76] can also be explored to lower the requirements on laser energy and so increase repetition rate. It is therefore feasible to generate laser-betatron or laser-ICS sources capable of image acquisition at frame rates of 100 f.p.s..

Table 1: Comparison of the properties of compact x-ray source technologies.

	Synchrotron	Compact commercial sources			High-power laser sources		
	TOMCAT beamline	MetalJet	Lyncean CLS	Mirrorcle	Laser-betatron	Laser-ICS	Laser-Kα
Photon energy and spectrum	$E_{crit} = 11.1$ keV (broadband), 8–45 keV (monochromatic, tunable)	15–35 keV[(a)] (24 keV In K$_\alpha$, 25 keV Sn K$_\alpha$ & broadband brems.)	15–35 keV (3% BW, tunable)	10–300 keV	5–100 keV[(e)] (broadband)	50–1000 keV (50% BW, tunable)	17.4 keV Kα
Source size (µm)	53×16	8	42	10	1	6	80
Divergence (mrad full angle)	2×0.6	227[(b)]	4[(c)]	50	10	10	4π sr
Photon flux (ph s^{-1} mrad^{-2})	3×10^{16} (broadband)	3.5×10^6 (in 15 – 35 keV BW)	2×10^9	3×10^{12}	6×10^6	10^5	10^5
Photons per pulse	–	–	–	5×10^{12}	10^{10}	10^6	10^{10}
Repetition rate	MHz	Continuous	65 MHz	400 Hz	$^1/_{20}$ Hz[(f)]	10 Hz	100 Hz
Photon rate (ph s^{-1})	10^{16}	10^{11}	3×10^{10}	2×10^{15}	5×10^8 [(f)]	10^7	10^{12}
Single-image exposure time	1 ms	0.6 s	$>$ 50 ms	–[(d)]	$<$ 100 fs	$<$ 100 fs	1 ps
1000-shot acquisition time	1 s	10 min	1 min	–[(d)]	5 hr[(f)]	100 s[(g)]	10 s
Reference	[15, 69]	[49]	[62, 63, 65]	[58]	[32, 33]	[70]	[48]

[(a)] MetalJet emits bremsstrahlung from 7 – 50 keV and has strong Ga K$_\alpha$ emission at 9 keV. When used for small animal imaging, the low energy x-rays are filtered by 210 μm Al to lower the dose.
[(b)] Metaljet emission angle is defined by the exit window. A 524 mrad window is also an option [excillum.com]
[(c)] CLS emission angle is defined by the design of the output mirror. 4 mrad is chosen as the best option for large field of view with a narrow bandwidth [62].
[(d)] Exposure and acquisition times for high resolution imaging (10 μm) are not reported. The scan time with 50 μm resolution is stated as 2 minutes [58] and exposure time for imaging a 30 cm object as 0.5 seconds [71].
[(e)] Beam characterisation and hard x-ray imaging is carried out after passage through an aluminium filter that cuts out photon energies below $\sim$ 5 keV.
[(f)] $^1/_{20}$ Hz is the repetition rate of the Gemini laser used in this study. Other lasers suitable for betatron generation are operational at 5 – 10 Hz.
[(g)] Tomographic imaging has not yet been reported. The 100 second value is a predicted scan time for 10 Hz operation.

5 Conclusion

X-ray pulses produced with laser-plasma accelerators can serve as compact sources for high resolution phase enhanced μCT scanning. Laser repetition rates up to 10 Hz are now available that could reduce the 3D acquisition time to less than a minute [77]. Compared to other high brightness compact x-ray sources the laser-betatron has the unique combination of $\sim 1\mu$m source size, straightforward scalability to high photon energies ($>$ 50 keV), and femtosecond pulse duration enabling blur-free imaging of any fast process. The laser-ICS scheme shares these properties and has a narrow bandwidth, although it is more complicated to implement and imaging of biological samples is yet to be demonstrated. A further advantage of the laser driver is that it can be expanded to generate other types of particles (electrons, ions, neutrons) and radiation (terahertz, UV, gamma rays) that are all intrinsically synchronised with the x-ray source. This technology could therefore be developed to construct dedicated machines providing a versatile imaging capability for the biological research sector.

6 Acknowledgements

The John Adams Institute is supported by the Science and Technology Facilities Council (ST/J002062/1, ST/P000835/1). We thank our collaborators and their teams for their contributions to the development of the laser-betatron souce for biological applications: S. Botchway (CLF); D. P. Norris (MRC Harwell Institute); L. Teboul (Mary Lyon Centre, MRC Harwell Institute); M. A. Hill (CRUK/MRC Oxford Institute for Radiation Oncology, University of Oxford).

References

[1] A. du Plessis et al. Laboratory x-ray micro-computed tomography: a user guideline for biological samples. *GigaScience* **6,** 6 (June 2017), pp. 1–11.

[2] R. A. Lewis. Medical phase contrast x-ray imaging: current status and future prospects. *Physics in Medicine and Biology* **49,** 16 (2004), p. 3573.

[3] A. Momose. Recent Advances in X-ray Phase Imaging. *Japanese Journal of Applied Physics* **44,** 9R (Sept. 2005), p. 6355.

[4] A. Bravin, P. Coan, and P. Suortti. X-ray phase-contrast imaging: from pre-clinical applications towards clinics. *Physics in Medicine and Biology* **58,** 1 (2013), R1.

[5] Y. Liu et al. Recent advances in synchrotron-based hard x-ray phase contrast imaging. *Journal of Physics D: Applied Physics* **46,** 49 (2013), p. 494001.

[6] T. Fiebig et al. Three-Dimensional In Vivo Imaging of the Murine Liver: A Micro-Computed Tomography-Based Anatomical Study. *PLoS ONE* **7,** 2 (Feb. 2012). Ed. by S. Afford, e31179.

[7] C. Honda and H. Ohara. Advantages of magnification in digital phase-contrast mammography using a practical X-ray tube. *European Journal of Radiology* **68,** 3 Suppl (Dec. 2008), pp. 69–72.

[8] I. Nesch et al. The design and application of an in-laboratory diffraction-enhanced x-ray imaging instrument. *The Review of Scientific Instruments* **80,** 9 (Sept. 2009), p. 093702.

[9] A. Momose et al. X-ray phase imaging: from synchrotron to hospital. *Phil. Trans. R. Soc. A* **372,** 2010 (Mar. 2014), p. 20130023.

[10] T. Koehler et al. Slit-scanning differential x-ray phase-contrast mammography: Proof-of-concept experimental studies. *Medical Physics* **42,** 4 (Apr. 2015), pp. 1959–1965.

[11] A. Tapfer et al. Experimental results from a preclinical X-ray phase-contrast CT scanner. *Proceedings of the National Academy of Sciences* **109,** 39 (Sept. 2012), pp. 15691–15696.

[12] O. Brunke et al. "Comparison between x-ray tube-based and synchrotron radiation-based μCT". Ed. by S. R. Stock. Vol. 7078. International Society for Optics and Photonics, Aug. 2008, 70780U.

[13] M. Kampschulte et al. Nano-Computed Tomography: Technique and Applications. *RoFo: Fortschritte Auf Dem Gebiete Der Rontgenstrahlen Und Der Nuklearmedizin* **188,** 2 (Feb. 2016), pp. 146–154.

[14] J. Moosmann et al. X-ray phase-contrast in vivo microtomography probes new aspects of Xenopus gastrulation. *Nature* **497,** 7449 (May 2013), pp. 374–377.

[15] R. Mokso et al. Four-dimensional in vivo X-ray microscopy with projection-guided gating. *Scientific Reports* **5,** (Mar. 2015), p. 8727.

[16] T. d. S. Rolo et al. In vivo X-ray cine-tomography for tracking morphological dynamics. *Proceedings of the National Academy of Sciences* **111,** 11 (Mar. 2014), pp. 3921–3926.

[17] S. Chang et al. Synchrotron x-ray imaging of pulmonary alveoli in respiration in live intact mice. *Scientific Reports* **5,** (Mar. 2015), p. 8760.

[18] L. Assoufid et al. Compact X-ray and extreme-ultraviolet light sources. *Optics and Photonics News* (July 2015).

[19] T. Tajima and J. M. Dawson. Laser Electron Accelerator. *Physical Review Letters* **43,** 4 (July 1979), pp. 267–270.

[20] V. Malka et al. Principles and applications of compact laser plasma accelerators. *Nature Physics* **4,** 6 (June 2008), pp. 447–453.

[21] E. Esarey, C. B. Schroeder, and W. P. Leemans. Physics of laser-driven plasma-based electron accelerators. *Reviews of Modern Physics* **81,** 3 (Aug. 2009), pp. 1229–1285.

[22] S. M. Hooker. Developments in laser-driven plasma accelerators. *Nature Photonics* **7,** 10 (Oct. 2013), pp. 775–782.

[23] X. Wang et al. Quasi-monoenergetic laser-plasma acceleration of electrons to 2 GeV. *Nature Communications* **4,** (June 2013), p. 1988.

[24] H. T. Kim et al. Enhancement of Electron Energy to the Multi-GeV Regime by a Dual-Stage Laser-Wakefield Accelerator Pumped by Petawatt Laser Pulses. *Physical Review Letters* **111,** 16 (Oct. 2013), p. 165002.

[25] W. Leemans et al. Multi-GeV Electron Beams from Capillary-Discharge-Guided Subpetawatt Laser Pulses in the Self-Trapping Regime. *Physical Review Letters* **113,** 24 (Dec. 2014), p. 245002.

[26] A. Rousse et al. Production of a keV x-ray beam from synchrotron radiation in relativistic laser-plasma interaction. *Physical Review Letters* **93,** 13 (Sept. 2004), p. 135005.

[27] S. Kneip et al. Bright spatially coherent synchrotron X-rays from a table-top source. *Nature Physics* **6,** 12 (Dec. 2010), pp. 980–983.

[28] S. Kneip, Z. Najmudin, and A. G. R. Thomas. A plasma wiggler beamline for 100 TW to 10 PW lasers. *High Energy Density Physics* **8,** 2 (June 2012), pp. 133–140.

[29] S. Corde et al. Femtosecond x rays from laser-plasma accelerators. *Reviews of Modern Physics* **85,** 1 (Jan. 2013), pp. 1–48.

[30] S. Cipiccia et al. Gamma-rays from harmonically resonant betatron oscillations in a plasma wake. *Nature Physics* **7,** 11 (Nov. 2011), pp. 867–871.

[31] J. Wenz et al. Quantitative X-ray phase-contrast microtomography from a compact laser-driven betatron source. *Nature Communications* **6,** May (2015), pp. 1–6.

[32] J. M. Cole et al. Laser-wakefield accelerators as hard x-ray sources for 3D medical imaging of human bone. *Scientific reports* **5,** (2015), p. 13244.

[33] J. M. Cole et al. High-resolution μCT of a mouse embryo using a compact laser-driven X-ray betatron source. *Proceedings of the National Academy of Sciences of the United States of America* **115,** 25 (June 2018), pp. 6335–6340.

[34] S. Fourmaux, J.-C. Kieffer, and A. Krol. "Ultrahigh resolution and brilliance laser wakefield accelerator betatron x-ray source for rapid in vivo tomographic microvasculature imaging in small animal models". Ed. by A. Krol and B. Gimi. Vol. 10137. International Society for Optics and Photonics, Mar. 2017, p. 1013715.

[35] D. P. Umstadter. All-laser-driven Thomson X-ray sources. *Contemporary Physics* **56,** 4 (Oct. 2015), pp. 417–431.

[36] H.-E. Tsai et al. Compact tunable Compton x-ray source from laser-plasma accelerator and plasma mirror. *Physics of Plasmas* **22,** 2 (Feb. 2015), p. 023106.

[37] K. Khrennikov et al. Tunable All-Optical Quasimonochromatic Thomson X-Ray Source in the Nonlinear Regime. *Physical Review Letters* **114,** 19 (May 2015), p. 195003.

[38] A. Döpp et al. Quick x-ray microtomography using a laser-driven betatron source. *Optica* **5,** 2 (Feb. 2018), p. 199.

[39] Z. Najmudin et al. Compact laser accelerators for X-ray phase-contrast imaging. *Phil. Trans. R. Soc. A* **372,** 2010 (Mar. 2014), p. 20130032.

[40] O. Hemberg, M. Otendal, and H. M. Hertz. Liquid-metal-jet anode electron-impact x-ray source. *Applied Physics Letters* **83,** 7 (2003), p. 1483.

[41] D. H. Larsson et al. A 24 keV liquid-metal-jet x-ray source for biomedical applications. *The Review of Scientific Instruments* **82,** 12 (Dec. 2011), p. 123701.

[42] O. Hemberg, M. Otendal, and H. M. Hertz. Liquid-metal-jet anode x-ray tube. *Optical Engineering* **43,** 7 (2004), p. 1682.

[43] D. Larsson. Small-Animal Imaging with Liquid-Metal-Jet X-Ray Sources. PhD thesis. KTH Royal Institute of Technology, 2015.

[44] R. Toth et al. In-line phase-contrast imaging with a laser-based hard x-ray source. *Review of Scientific Instruments* **76,** 8 (Aug. 2005), p. 083701.

[45] S. Fourmaux and J. C. Kieffer. Laser-based K α X-ray emission characterization using a high contrast ratio and high-power laser system. *Applied Physics B* **122,** 6 (June 2016), p. 162.

[46] G. Korn et al. Ultrashort 1-kHz laser plasma hard x-ray source. *Optics Letters* **27,** 10 (May 2002), pp. 866–868.

[47] C. M. Laperle et al. Propagation based differential phase contrast imaging and tomography of murine tissue with a laser plasma x-ray source. *Applied Physics Letters* **91,** 17 (2007), p. 173901.

[48] Y. Azamoum et al. High photon flux Kα Mo x-ray source driven by a multi-terawatt femtosecond laser at 100 Hz. *Optics Letters* **43,** 15 (Aug. 2018), p. 3574.

[49] D. H. Larsson et al. High-resolution short-exposure small-animal laboratory x-ray phase-contrast tomography. *Scientific Reports* **6,** (Dec. 2016), p. 39074.

[50] T. Tuohimaa, M. Otendal, and H. M. Hertz. Phase-contrast x-ray imaging with a liquid-metal-jet-anode microfocus source. *Applied Physics Letters* **91,** 7 (Aug. 2007), p. 074104.

[51] D. H. Larsson et al. First application of liquid-metal-jet sources for small-animal imaging: High-resolution CT and phase-contrast tumor demarcation. *Medical Physics* **40,** 2 (Feb. 2013), p. 021909.

[52] T. Thüring et al. X-ray grating interferometry with a liquid-metal-jet source. *Applied Physics Letters* **103,** 9 (Aug. 2013), p. 091105.

[53] M. Preissner et al. High resolution propagation-based imaging system for in vivo dynamic computed tomography of lungs in small animals. *Physics in Medicine & Biology* **63,** 8 (Apr. 2018), 08NT03.

[54] W. Vågberg et al. X-ray phase-contrast tomography for high-spatial-resolution zebrafish muscle imaging. *Scientific Reports* **5,** (Nov. 2015), p. 16625.

[55] M. Töpperwien et al. Phase-contrast tomography of neuronal tissues: from laboratory- to high resolution synchrotron CT. *Proc. SPIE 9967, Developments in X-Ray Tomography X* (2016), 99670T.

[56] H. Yamada. Novel X-ray source based on a tabletop synchrotron and its unique features. *Nuclear Instruments and Methods in Physics Research Section B: Beam Interactions with Materials and Atoms* **199,** (2003), p. 509.

[57] J. van Heekeren et al. Characterization of an x-ray phase contrast imaging system based on the miniature synchrotron MIRRORCLE-6X. *Medical Physics* **38,** 9 (Sept. 2011), pp. 5136–5145.

[58] H. Yamada et al. "Tabletop Synchrotron Light Source". *Comprehensive Biomedical Physics*. Ed. by A. Brahme. Vol. 8. Amsterdam: Elsevier, 2014, pp. 43–65.

[59] Z. Huang and R. D. Ruth. Laser-Electron Storage Ring. *Physical Review Letters* **80,** 5 (Feb. 1998), pp. 976–979.

[60] R. J. Loewen. A compact light source: design and technical feasibility study of a laser-electron storage ring X-ray source. PhD thesis. Stanford University Stanford CA, 2003.

[61] W. Graves et al. Compact x-ray source based on burst-mode inverse Compton scattering at 100 kHz. *Physical Review Special Topics - Accelerators and Beams* **17,** 12 (Dec. 2014), p. 120701.

[62] E. Eggl et al. The Munich Compact Light Source: initial performance measures. *Journal of Synchrotron Radiation* **23,** 5 (Sept. 2016), pp. 1137–1142.

[63] B. Gunther et al. The Munich Compact Light Source: Flux Doubling and Source Position Stabilization At a Compact Inverse-Compton Synchrotron X-ray Source. *Microscopy and Microanalysis* **24,** S2 (Aug. 2018), pp. 316–317.

[64] E. Eggl et al. X-ray phase-contrast tomography with a compact laser-driven synchrotron source. *Proceedings of the National Academy of Sciences* **112,** 18 (May 2015), pp. 5567–5572.

[65] R. Gradl et al. Propagation-based Phase-Contrast X-ray Imaging at a Compact Light Source. *Scientific Reports* **7,** 1 (Dec. 2017), p. 4908.

[66] R. Gradl et al. In vivo Dynamic Phase-Contrast X-ray Imaging using a Compact Light Source. *Scientific Reports* **8,** 1 (Dec. 2018), p. 6788.

[67] M. Bech et al. Hard X-ray phase-contrast imaging with the Compact Light Source based on inverse Compton X-rays. *Journal of Synchrotron Radiation* **16,** 1 (Jan. 2009), pp. 43–47.

[68] K. Achterhold et al. Monochromatic computed tomography with a compact laser-driven X-ray source. *Scientific Reports* **3,** (2013), p. 1313.

[69] M. Stampanoni et al. Trends in synchrotron-based tomographic imaging: the SLS experience. *Proc. SPIE 6318, Developments in X-Ray Tomography V* (2006), p. 63180M.

[70] N. D. Powers et al. Quasi-monoenergetic and tunable X-rays from a laser-driven Compton light source. *Nature Photonics* **8,** 1 (Jan. 2014), pp. 28–31.

[71] H. Yamada et al. Portable synchrotron hard X-ray source MIRRORCLE-6x for X-ray imaging. *Proc. 8th Int. Conf. X-ray Microscopy, IPAP Conf. Series 7* (2005), pp. 130–132.

[72] C. Danson et al. Petawatt class lasers worldwide. *High Power Laser Science and Engineering* **3,** (Jan. 2015), E3.

[73] C. L. Haefner et al. "High average power, diode pumped petawatt laser systems: a new generation of lasers enabling precision science and commercial applications". Ed. by G. Korn and L. O. Silva. Vol. 10241. International Society for Optics and Photonics, June 2017, p. 1024102.

[74] P. Mason et al. Kilowatt average power 100 J-level diode pumped solid state laser. *Optica* **4,** 4 (Apr. 2017), pp. 438–439.

[75] S. M. Hooker et al. Multi-pulse laser wakefield acceleration: a new route to efficient, high-repetition-rate plasma accelerators and high flux radiation sources. *Journal of Physics B: Atomic, Molecular and Optical Physics* **47,** 23 (2014), p. 234003.

[76] J. Cowley et al. Excitation and Control of Plasma Wakefields by Multiple Laser Pulses. *Physical Review Letters* **119,** 4 (July 2017), p. 044802.

[77] J. Götzfried et al. Research towards high-repetition rate laser-driven X-ray sources for imaging applications. *Nuclear Instruments and Methods in Physics Research, Section A: Accelerators, Spectrometers, Detectors and Associated Equipment* **909,** (Nov. 2018), pp. 286–289.